

# Random-field-driven phase transitions in the ground state of the $S = 1$ $XXZ$ spin chain

Yoshihiro Nishiyama

*Department of Physics, Faculty of Science, Okayama University  
Okayama 700, Japan*

(Received )

## Abstract

Ground-state of the  $S = 1$   $XXZ$  spin chain under the influence of the random magnetic field is studied by means of the exact-diagonalization method. The  $S = 1/2$  counterpart has been investigated extensively so far. The easy-plane area, including the Haldane and the  $XY$  phases, is considered. The area suffers significantly from the magnitude of the constituent spin. Destruction of the Haldane state is observed at a critical strength of the random field, which is comparable to the magnitude of the Haldane gap. This transition is characterized by the disappearance of the string order. The  $XY$  region continues until at a critical randomness, at which a transition of the KT-universality class occurs. These features are contrasted with those of the  $S = 1/2$  counterpart.

## 1 Introduction

In *quantum* statistical mechanics, randomnesses still remain non-trivial, even though they do not introduce any competing interactions. The essence of the integer quantum hole effect, for example, is attributed to the randomness-driven localization-delocalization transition under the presence of high magnetic field. Although this description is simply of the one-body picture, it is very hard to

deal with this problem. The effect of randomness for the quantum *many-body* system would be more complicated, and has not been investigated very well. In order to consider the effect of randomness for such the systems as the Mott insulator and the superconductor, for example, it is significant to take into account of the many-body interactions [1].

In one dimension, some analytic treatments are available: The random  $S = 1/2$   $XXZ$  model was investigated with the bosonization technique [2] and the real-space decimation method [3]. The real-space decimation method yields comprehensive understanding of the random transverse-field Ising chain as well [4, 5]. The analytical predictions of these theories are confirmed numerically [6, 7, 8, 9]. In the course of the above studies, one could resort to very nice and special mathematical characteristics. That is, the  $S = 1/2$  chain is described in the language of the bosonization formalism, while the transverse-field Ising chain is related to the free-fermion model with the Jordan-Wigner transformation. Because both the resultant models are understood very well, the effect of the randomness could be considered to a certain extent.

Recently, more general systems, which are possibly missing such the nice characteristics as above, have been attracting considerable attention [10, 11, 12, 13, 14, 15, 16, 17]. It is suggestive that the real-space decimation method fails for the cases other than  $S = 1/2$  [3, 13]. This is somehow consistent with the Haldane conjecture [18], which states that the quantum magnet is affected by the magnitude of the spin quantitatively. According to his conjecture, the ground state of the  $S = 1$  chain is massive. Hence, in this case, the technique [2, 19, 20] based on the bosonization formalism fails as well. Few studies have been reported for the  $S = 1$  magnet so far [10, 12, 13, 14, 16]. These studies are concerned in the bond-random  $S = 1$  Heisenberg magnet.

Here, we study the  $S = 1$   $XXZ$  model with the random magnetic field,

$$\mathcal{H} = \sum_{i=1}^L (S_i^x S_{i+1}^x + S_i^y S_{i+1}^y + \lambda S_i^z S_{i+1}^z + H_i S_i^z). \quad (1)$$

The operators  $\{\mathbf{S}_i\}$  denote the  $S = 1$  spin operators acting on the

site  $i$ . The random field  $\{H_i\}$  distributes uniformly over the range  $[-\sqrt{3}\Delta, \sqrt{3}\Delta]$ . Therefore the mean deviation is given by  $\sqrt{[H_i^2]_{\text{av}}} = \Delta$ .

Under the absence of the random field  $\Delta = 0$ , the ground state phase diagram of the system (1) is known [21, 22]: (It is noteworthy that the phase diagram is different qualitatively from that of the  $S = 1/2$  chain, which is reviewed in the next section.) In the region  $\lambda < -1$ , the ground state is ferromagnetic. In the region  $-1 < \lambda < 0$ , the ground state is in the  $XY$  phase. Therefore, in this area, the ground-state magnetic correlation decays obeying the power law,

$$\langle S_i^x S_j^x \rangle \sim 1/|i - j|^{\eta_{S=1}}. \quad (2)$$

The exponent  $\eta_{S=1}$  is speculated to [23] be described by the formula,

$$\eta_{S=1} = \frac{\pi - \cos^{-1} \lambda}{2\pi}. \quad (3)$$

In the region  $0 < \lambda < 1.2 \dots$ , the Haldane phase extends. In the Haldane phase, The ground state is massive, and the magnetic correlation decays exponentially,

$$\langle S_i^x S_j^x \rangle \sim e^{-|i - j|/\xi}. \quad (4)$$

At the isotropic point  $\lambda = 1$ , the Haldane gap  $\Delta E_{\text{triplet}}$  and the correlation length  $\xi$  are estimated numerically [24];  $\Delta E_{\text{triplet}} = 0.41049(2)$  and  $\xi = 6.2$ , respectively. The antiferromagnetic phase appears in the remaining region  $1.2 \dots < \lambda$ . Among the above four phases, the antiferromagnetic and the ferromagnetic phases are of rather classical nature. Hence, in this paper, we devote ourselves to the easy-plane region, namely, the Haldane and the  $XY$  phases. Both phases are realized precisely due to the quantum effect, and the influence of the randomness is unclear.

The present paper is organized as follows. First, we review the results obtained for the  $S = 1/2$  model in the next section. In Section 3, our numerical results for the  $S = 1$  chain (1) are presented. First, we focus on the transition from the Haldane phase to the localization phase at the isotropic point  $\lambda = 1$ . For the first time, we observed the onset of the localization transition from the Haldane

phase at  $\Delta_c = 0.49 \pm 0.15$ , with the critical exponent  $\nu = 3.4 \pm 2.2$ . The transition is characterized as the disappearance of the string correlation. In the remaining part, we concentrate on the  $XY$  region  $-1 < \lambda < 0$ . We find that the  $XY$  phase persists considerably against the randomness, and the randomness-riven phase transition is of the KT universality class. In the last section, we summarize these results, and make a comparison between ours and those of  $S = 1/2$ .

## 2 Review — the ground-state phase diagram and the criticality of the $S = 1/2$ $XXZ$ chain with the random magnetic field

Here, we summarize the ground-state property of the the Hamiltonian (1) in the case of  $S = 1/2$ . First, we explain the phase-diagram without randomness [25, 26]: the  $XY$  phase spans the whole easy-plane region  $-1 < \lambda < 1$ . In this  $XY$  phase, the critical exponent  $\eta_{S=1/2}$  is evaluated exactly [27] as the function of the anisotropy  $\lambda$ ,

$$\eta_{S=1/2} = \frac{\pi - \cos^{-1} \lambda}{\pi}. \quad (5)$$

Beside this  $XY$  phase, the ferromagnetic phase appears in  $\lambda < -1$ , while the antiferromagnetic phase extends in  $1 < \lambda$ .

The ground-state phase diagram in the presence of the random field is depicted in Fig. 1. The diagram is determined with various means, the bosonization technique [2], real-space decimation method [3] and the exact-diagonalization method [8].

If a ground state is critical and the critical exponent  $\eta$  is known, Harris's criterion [28] tells whether randomness is a relevant perturbation or not. The Harris criterion in the present case [2] states that the random-field perturbation is relevant (irrelevant), if the exponent is  $\eta > 1/3$  ( $\eta < 1/3$ ); and so,  $\eta_c = 1/3$ . Note that this criterion together with the formula (5) yields the conclusion consistent to the phase diagram shown in Fig. 1; the  $XY$  phase is stable in the anisotropy range  $-1 < \lambda < -0.5$ , whereas it is unstable in the other range  $-0.5 < \lambda < 1$ .

The criterion, however, is concerned only with the vicinity of the line  $\Delta = 0$ . Hence, we must resort to numerical simulations in order to investigate the region of the finite randomness  $\Delta > 0$ . The phase diagram of the full range of the randomness was explored by means of the numerical simulation by Runge and Zimanyi [8]. In our case  $S = 1$ , there also appears the Haldane phase, which is driven out of a certain criticality. Therefore, no rigorous criterion such as Harris's is available even in the vicinity of the pure line. These are the reasons why we managed the numerical simulation.

Lastly, we mention physical interpretation of the phase diagram. The  $S = 1/2$  magnet is transformed with the Jordan-Wigner transformation to the spinless-fermion system,

$$\mathcal{H}_{\text{sf}} = \sum_i \left\{ 0.5(c_i^\dagger c_{i+1} + \text{h.c.}) + \lambda(c_i^\dagger c_i - 1/2)(c_{i+1}^\dagger c_{i+1} - 1/2) + 0.5H_i c_i^\dagger c_i \right\}. \quad (6)$$

In consequence, we see that the parameter  $\lambda$  controls the strength of the repulsion among the particles, and the randomness  $\Delta$  enters as the potential randomness. In general, the particles become stable against the randomness as the cohesive force is strengthened; the tendency is quite consistent with the phase diagram in Fig. 1.

### 3 Numerical results

In this section, we investigate the ground state of the model (1) by means of the exact-diagonalization method. The results for the Haldane and the  $XY$  phases are presented separately in respective subsections. In the subsections 3.1 and 3.2, each data is averaged over 128 and 160 samples, respectively. The diagonalization was performed within the sub-space of the quantum number  $\sum_i^L S_i^z = 0$ . This sub-space is the most relevant to the ground-state: In fact, at  $\Delta = 0$ , the ground state belongs to this subspace. This would not be violated essentially even in the presence of finite randomnesses  $\Delta > 0$  because of the symmetry of the Hamiltonian (1) under the transformation  $z \leftrightarrow -z$ .

### 3.1 Random-field driven phase transition from the Haldane phase

As is explained in Section 1, in the region  $0 < \lambda < 1.2 \cdots$  ( $\Delta = 0$ ), the Haldane phase is realized. At the isotropic point  $\lambda = 1$ , the magnitude of the Haldane gap becomes maximal. Here, we concentrate on this point  $\lambda = 1$ .

Some might wonder that the Haldane phase and the localization (random-field) phase are equivalent, because they both exhibit short-range magnetic correlations. Here, however, we show for the first time that these phases are distinguishable, in other words, a critical point separates these phases.

In order to discriminate the phases, we utilized the string correlation [29, 30],

$$\mathcal{O}_{\text{string}}^x(j-i) = \left[ \left\langle S_i^x e^{i\pi \sum_{k=i}^{j-1} S_k^x} S_j^x \right\rangle \right]_{\text{av}}. \quad (7)$$

Here, the bracket  $\langle \rangle$  denotes the ground-state expectation value, and the symbol  $[ ]_{\text{av}}$  stands for the random average. The string order develops [31] in the ground state of the Haldane phase, although the usual magnetic correlation is short-ranged; see eq. (4).

Because of the presence of the random field parallel to the  $z$  axis, the  $z$ -component correlation is suffered from the random-field disturbance directly. Hence, we have evaluated the  $x$ -component correlation, as is defined in eq. (7). (In the numerical simulation, such a off-diagonal operator is more difficult to treat than the diagonal one. This difficulty limited the maximal system size and the number of samples available.)

In Fig. 2, we plotted the Binder parameter [32] associated with the string correlation (7),

$$U_{\text{string}} = 1 - \frac{\langle M_{\text{string}}^4 \rangle}{3 \langle M_{\text{string}}^2 \rangle^2}, \quad (8)$$

where the string-order magnetization is given by,

$$M_{\text{string}} = \sum_{i=1}^L S_i^x e^{i\pi \sum_{k=1}^{i-1} S_k^x}. \quad (9)$$

As the system size is increased, the Binder parameter approaches to 2/3, if the corresponding order, namely, the string order, develops. On the other hand, it vanishes in the disorder region, as the system size is enlarged. It is system-size invariant at the critical point. Actually, we see in Fig. 2, that in the region  $\Delta < 0.5$  the Binder parameter grows through enlarging the system size, while it is suppressed in the opposite area  $0.5 < \Delta$ . In consequence, we see that the Haldane phase persists against the randomness up to  $\Delta_c \sim 0.5$ , whereas it is disturbed by the random field in the region  $\Delta > 0.5$ .

In order to investigate the criticality more precisely, we employed the finite-size-scaling technique. The finite-size-scaling theory tells that a dimensionless quantity such as the Binder parameter should be described by the formula,

$$U(L) = \tilde{U}(L/\xi). \quad (10)$$

The correlation length diverges in the vicinity of the critical point  $\Delta_c$  in the form,

$$\xi = |\Delta - \Delta_c|^{-\nu}, \quad (11)$$

where  $\nu$  is the correlation-length critical exponent. As a consequence, the  $[(\Delta - \Delta_c)L^{1/\nu}]$ - $U$  plots should form an universal curve irrespective to the system size  $L$ . In other words, the scaling parameters, such as  $\Delta_c$  and  $\nu$ , are chosen so that the plots, the so-called scaling plots, align all along a curve. The degree of the alignment is measured in the way explained in Appendix A.

The scaling plot is presented in Fig. 3. The plot determined the critical randomness  $\Delta_c = 0.49 \pm 0.15$  and the critical exponent  $\nu = 3.4 \pm 2.2$ . We find that the magnitude of the critical point is comparable with the magnetic excitation gap  $\Delta E_{\text{triplet}} = 0.41049(2)$  [24] at the condition  $\Delta = 0$  and  $\lambda = 1$ .

### 3.2 Random-field-driven transition from the $XY$ phase

Here we investigate the  $XY$  phase  $-1 < \lambda < 0$ . The  $XY$  phase is characterized by the presence of the spin stiffness [33],

$$\rho_s = L \left[ \left\langle \frac{\partial^2 E_0(\theta)}{\partial \theta^2} \right\rangle \right]_{\text{av}}. \quad (12)$$

The symbol  $E_0(\theta)$  denotes the ground state energy, and the angle  $\theta$  is associated with the gauge twist of the boundary condition;  $S_L^+ S_1^- \rightarrow e^{i\theta} S_L^+ S_1^-$ . In other words, the spin stiffness measures the long-range coherence of the gauge symmetry, and thus it is related to the superfluid density in the context of the electron system. The spin stiffness should vanish in the localization (random-field) phase, because the global coherence is destructed there.

In Fig. 4, we plotted the spin stiffness against the randomness. The stiffness is suppressed, as the randomness is strengthened. In the weak-random region  $\Delta < 1$ , the stiffness hardly changes with respect to the system size. Hence, we observe in this area, the stiffness remains finite in the thermodynamic limit; that is, in this region, the  $XY$  phase is realized. In the area  $\Delta > 1$ , however, the stiffness vanishes rapidly through enlarging the system size. Each spin is enforced to point towards the random-field direction; the localization phase is realized there. To summarize, we see that the  $XY$  phase persists up to the critical randomness  $\Delta_c \sim 1$ , and beyond the threshold the ground state becomes localized.

We explore the criticality with the finite-size-scaling method. Because the stiffness is system-size invariant at the critical point, the stiffness is described by the formula,

$$\rho_s = \tilde{\rho}_s(L/\xi). \quad (13)$$

(Note that it is identical with the form for the Binder parameter (10).) The correlation length  $\xi$  would obey the KT type form,

$$\xi \sim e^{A/\sqrt{\Delta - \Delta_c}}, \quad (14)$$

because a finite critical region extends as is shown above.

The scaling data for  $\lambda = -0.5$  is presented in Fig. 5. This plot yields the estimates  $\Delta_c = 0.85 \pm 0.30$  and  $A \sim 0.65$ . (For the details of the analysis, refer to Appendix A.)

In order to confirm the above result, we show another analysis for determining the transition point. As is reviewed in Section 2, the Harris criterion insists that the correlation decays with the exponent  $\eta_c = 1/3$  at the localization-delocalization transition point. In order to adopt this criterion, we plotted the log-log plot of the square of

the normalized staggered magnetization,

$$M_{\text{stg}}^2/L^2 = 1/L^2 \left( \sum_i (-1)^i S_i^x \right)^2 \sim 1/L^\eta, \quad (15)$$

for various randomnesses in Fig. 6. We observe that the above criterion yields the estimate  $\Delta_c \sim 1$ . This conclusion is consistent with the former estimate  $\Delta_c = 0.85 \pm 0.30$ . The agreement would be satisfactory.

Secondly, we present the results at the condition  $\lambda = 0$ ; see Figs. 7-9. The results resemble those of  $\lambda = -0.5$ : The scaling analysis for the spin stiffness yields the critical point  $\Delta_c = 0.87 \pm 0.30$  (see Fig. 8), whereas the Harris criterion suggests that  $\Delta_c \sim 1$  (see Fig. 9). Again, both estimates are in good agreement.

Lastly, we show the results for  $\lambda = -1$ ; see Figs. 10-12. (We found that in the range  $\Delta > 0.6$  of  $L = 14$ , diagonalization convergence is hardly achieved for some random samples. Hence, the corresponding data are missing in these figures.) We observe in Fig. 10 that solely at  $\Delta = 0$ , *XY* state is realized, and for the region other than that, the localization phase is realized. In fact, we find that the data is scaled well under the assumption of the formula (11); see Fig. 11. The analysis gives the criticality  $\Delta_c = -0.13 \pm 0.10$  and  $\nu = 0.70 \pm 0.10$ . The negative value of the randomness is apparently non-sense. Considering a certain statistical error, we suspect that the transition point is located at  $\Delta \sim 0$ . The Harris criterion, see Fig. 12, confirms this conclusion: In the figure, it is shown clearly that the correlation is suppressed owing to the randomness significantly. That is, all the data are curved convexly. This fact suggests that the correlation decays exponentially even for the infinitesimal randomness.

## 4 Summary and discussions

We have investigated the  $S = 1$  *XXZ* chain with the random magnetic field (1) by means of the exact-diagonalization method. To summarize our numerical results presented in Section 3, we depicted a drawing of the ground-state phase diagram as in Fig. 13. This

diagram should be contrasted to that of the  $S = 1/2$  model shown in Fig. 1.

First, we discuss the Haldane phase ( $\lambda = 1$ ). Although both the Haldane and the random-field phase are magnetically disordered, these phases are separated distinctively by the phase boundary. The Haldane phase is characterized by the presence of the string order (7), whereas the localization phase is missing the order. We found that the phase boundary is located at the random-field strength  $\Delta_c = 0.49 \pm 0.15$ . It is noteworthy that this critical value is comparable with the magnitude of the Haldane gap,  $\Delta E_{\text{triplet}} = 0.41049(2)$  [24]. Moreover, we obtained the critical exponent  $\nu = 3.4 \pm 2.2$  with the finite-size-scaling analysis. At present, little is reported on the ground-state criticality driven by *randomness* on related systems: In the case of  $S = 1/2$  at the isotropic point  $\lambda = 1$ , the localization-delocalization transition occurs at  $\Delta_c = 0$  with the exponent  $\nu = 1$  [3, 8]. Our universality class would not be identical to this, and possibly unique.

Lastly, we mention the  $XY$  phase ( $-1 < \lambda < 0$ ). The phase boundary is determined both by the scaling plot of the spin stiffness and the Harris criterion on the correlation-decay rate. Both estimates are in good agreement. We observed that the whole region  $-1 < \lambda < 0$  is stable against the randomness, and the phase boundary extends up to the random strength  $\Delta \sim 0.9$ . Note that in the case of  $S = 1/2$ , the  $XY$  phase is stable only in the range  $-1 < \lambda < -0.5$ , and furthermore the maximal critical randomness is  $\sim 0.12$  at most. These maximal critical randomnesses are far apart. Even if we normalize the energy unit in terms of the magnitude of the respective spins, the discrepancy between these estimates is not resolved completely. We conjecture that through enlarging the magnitude of the constituent spin, classical nature emerges very rapidly. That is to say, for a large-spin chain, the ground-state magnetism is very stable in respect to the randomness. This consequence is quite reasonable, because classical magnetic order survives even in the presence of the random field at the ground state.

We have not dealt with the region a bit exceeding the point  $\lambda = 0$ . At this point ( $\Delta = 0$ ), the KT transition takes place; The energy

gap starts to open *very slowly*. Hence, severe correction [34] to the finite-size scaling emerges. This difficulty is remained to be solved for the future.

## Acknowledgement

Our computer programs are partly based on the subroutine package “TITPACK Ver. 2” coded by Professor H. Nishimori. Numerical simulations were performed on the parallel supercomputers FUJITSU VPP700/56 of the computer center, Kyushu university.

## A Details of the present scaling analyses

We explain the details of our finite-size-scaling analyses, which we managed in Section 3 in order to estimate the transition point  $\Delta_c$ , the exponent  $\nu$  in eq. (11), and the coefficient  $A$  in eq. (14). We adjusted these scaling parameters so that the scaled data, such as those shown in Figs. 3 and 5, form a curve irrespective of the system sizes. In order to see quantitatively to what extent these data align, we employ the “local linearity function”  $S$  defined by Kawashima and Ito [35]: Suppose a set of the data points  $\{(x_i, y_i)\}$  with the errorbar  $\{d_i (= \delta y_i)\}$ , which we number so that  $x_i < x_{i+1}$  may hold for  $i = 1, 2, \dots, n - 1$ . For this data set, the local-linearity function is defined as

$$S = \sum_{i=2}^{n-1} w(x_i, y_i, d_i | x_{i-1}, y_{i-1}, d_{i-1}, x_{i+1}, y_{i+1}, d_{i+1}). \quad (16)$$

The quantity  $w(x_j, y_j, d_j | x_i, y_i, d_i, x_k, y_k, d_k)$  is given by

$$w = \left( \frac{y_j - \bar{y}}{\Delta} \right)^2, \quad (17)$$

where

$$\bar{y} = \frac{(x_k - x_j)y_i - (x_i - x_j)y_k}{x_k - x_i} \quad (18)$$

and

$$\Delta^2 = d_j^2 + \left( \frac{x_k - x_j}{x_k - x_i} d_i \right)^2 + \left( \frac{x_i - x_j}{x_k - x_i} d_k \right)^2. \quad (19)$$

In other words, the numerator  $y_j - \bar{y}$  denotes the deviation of the point  $(x_j, y_j)$  from the line passing two points  $(x_i, y_i)$  and  $(x_k, y_k)$ , and the denominator  $\Delta$  stands for the statistical error of  $(y_i - \bar{y})$ . And so,  $w = ((y_i - \bar{y})/\Delta)^2$  shows a degree to what extent these three points align. The advantage in the above analysis is as follows: In the conventional least square fitting, we need to assume some particular fitting function. The assumption which function we use causes systematic error. Note that in the present analysis, we do not have to assume any fitting functions.

The scaling parameters are determined so as to minimize the local-linearity function. The error margin of the scaling parameter is hard to estimate. It is concerned with both the statistical error and the correction to the finite size scaling. The former error can be estimated through considering the statistical error of the function  $S$ . This function has a relative error of the order  $1/\sqrt{n-2}$ . (The local-linearity function is of the order  $(n-2)$ , and the error is given by  $\sqrt{n-2}$ .) The correction to the finite-size scaling, on the contrary, is quite difficult to determine. In the present study, in particular, the KT transition occurs. In that case, in general, the correction to the finite-size scaling emerges severly. Here, we consider only the statistical error in order to estimate the error margins of the scaling parameters. As the number of the data points  $n$  is increased, the statistical error of  $S$  would be reduced. The corrections to the finite-size scaling might increase instead. In the present analyses, we used twenty data in the vicinity of the transition point  $\Delta_c$ . An example of the plot  $S$  is shown in Fig. 14. We observe the minimum at  $\nu \approx 1.5$ . Taking into account of the statistical error, we estimated the critical exponent as  $\nu = 3.4 \pm 2.2$ .

## References

- [1] M. P. A. Fisher, P. B. Weichman, G. Grinstein and D. S. Fisher: Phys. Rev. B **40** (1989) 546.
- [2] C. A. Dory and D. S. Fisher: Phys. Rev. B **45** (1992) 2167.
- [3] D. S. Fisher: Phys. Rev. B **50** (1994) 3799.

- [4] D. S. Fisher: Phys. Rev. Lett. **69** (1992) 534.
- [5] D. S. Fisher: Phys. Rev. B **51** (1995) 6411.
- [6] N. Nagaosa: J. Phys. Soc. Jpn. **56** (1987) 2460.
- [7] S. Haas, J. Riera and E. Dagotto: Phys. Rev. B **48** (1993) 13174.
- [8] K. J. Runge and G. T. Zimanyi: Phys. Rev. B **49** (1994) 15212.
- [9] A. P. Young and H. Rieger: Phys. Rev. B **53** (1996) 8486.
- [10] B. Boechat, A. Saguia and M. A. Continentino: Solid State Communications **98** (1996) 411.
- [11] R. A. Hyman, K. Yang, R. N. Bhatt and S. M. Girvin: Phys. Rev. Lett. **76** (1996) 839.
- [12] K. Yang, R. A. Hyman, R. N. Bhatt and S. M. Girvin: J. Appl. Phys. **79** (1996) 5096.
- [13] R. A. Hyman and K. Yang: Phys. Rev. Lett. **78** (1997) 1783.
- [14] C. Monthus, O. Golinelli and T. Jolicoeur: Phys. Rev. Lett. **79** (1997) 3254.
- [15] K. Hida: J. Phys. Soc. Jpn. **66** (1997) 3237.
- [16] Y. Nishiyama: to appear in Physica A.
- [17] S. Todo: preprint.
- [18] F. D. M. Haldane: Phys. Lett. **93A** (1983) 464.
- [19] T. Gimarchi and H. J. Schulz: Europhys. Lett. **3** (1987) 1287.
- [20] T. Gimarchi and H. J. Schulz: Phys. Rev. B **37** (1988) 325.
- [21] H. J. Schulz: Phys. Rev. B **34** (1986) 6372.
- [22] T. Sakai and M. Takahashi: J. Phys. Soc. Jpn. **59** (1990) 2688.
- [23] F. C. Alcaraz and A. Moreo: Phys. Rev. B **46** (1992) 2896.

- [24] O. Golinelli, Th. Jolicœur and R. Lacaze: Phys. Rev. B **50** (1994) 3037.
- [25] C. N. Yang and C. P. Yang: Phys. Rev. **150** (1966) 321.
- [26] C. N. Yang and C. P. Yang: Phys. Rev. **150** (1966) 327.
- [27] R. J. Baxter: Ann. Phys. (N. Y.) **70** (1972) 323.
- [28] A. B. Harris: J. Phys. **C 7** (1974) 1671.
- [29] M. den Nijs and K. Rommelse: Phys. Rev. B **40** (1989) 4709.
- [30] H. Tasaki: Phys. Rev. Lett. **66** (1991) 798.
- [31] S. M. Girvin and D. P. Arovas: Phys. Scr. **T27** (1989) 156.
- [32] K. Binder: Phys. Rev. Lett. **47** (1981) 693.
- [33] M. E. Fisher, M. N. Barber and D. Jasnow: Phys. Rev. A **8** (1973) 1111.
- [34] A. L. Malvezzi and F. C. Alcaraz: J. Phys. Soc. Jpn. **64** (1995) 4485.
- [35] N. Kawashima and N. Ito: J. Phys. Soc. Jpn. **62** (1993) 435.

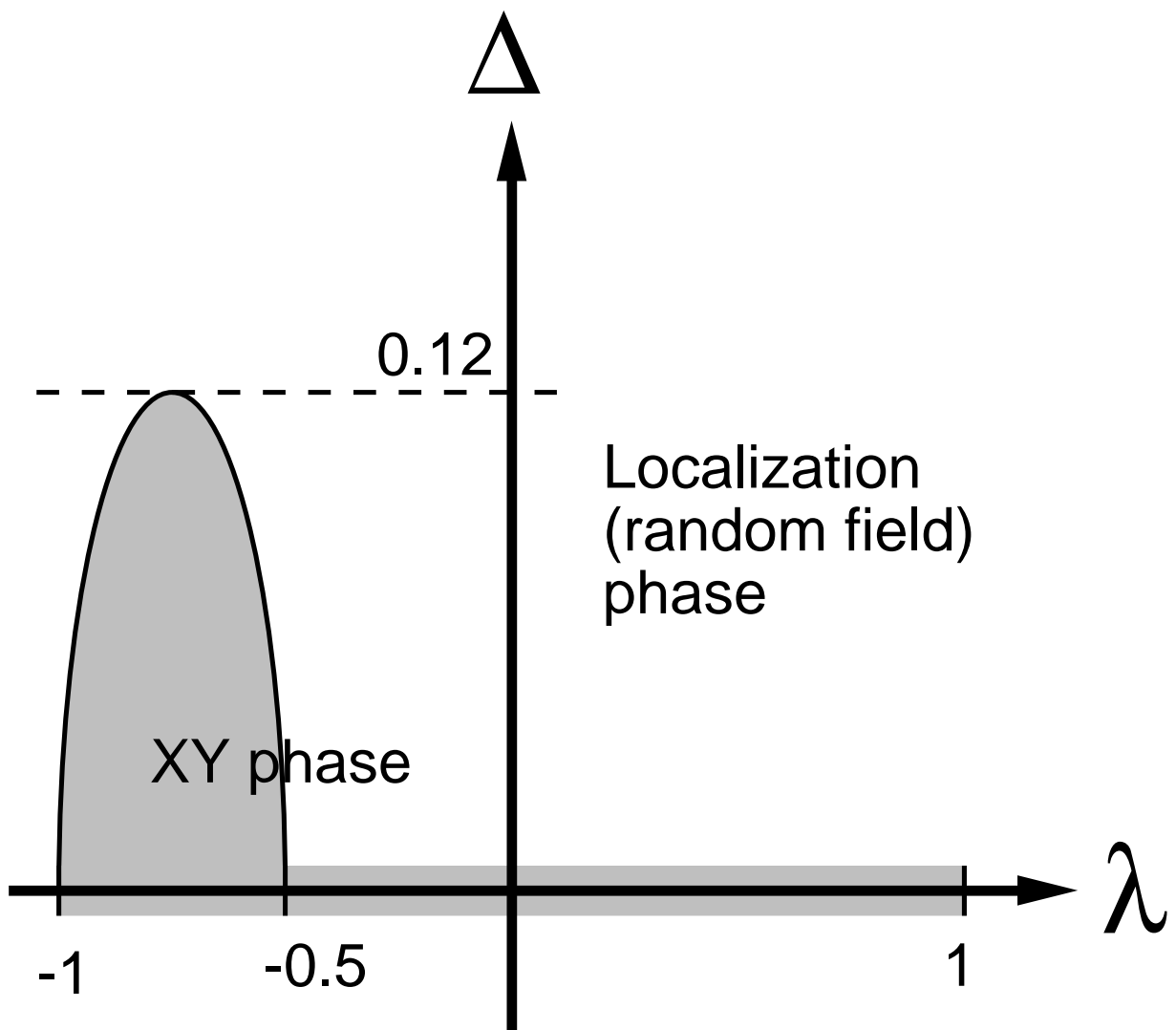


Figure 1: The ground-state phase diagram of the  $S = 1/2$  XXZ model (1) under the presence of the random magnetic field  $\Delta$ . Here, we have referred to the figure appearing in the article [8].

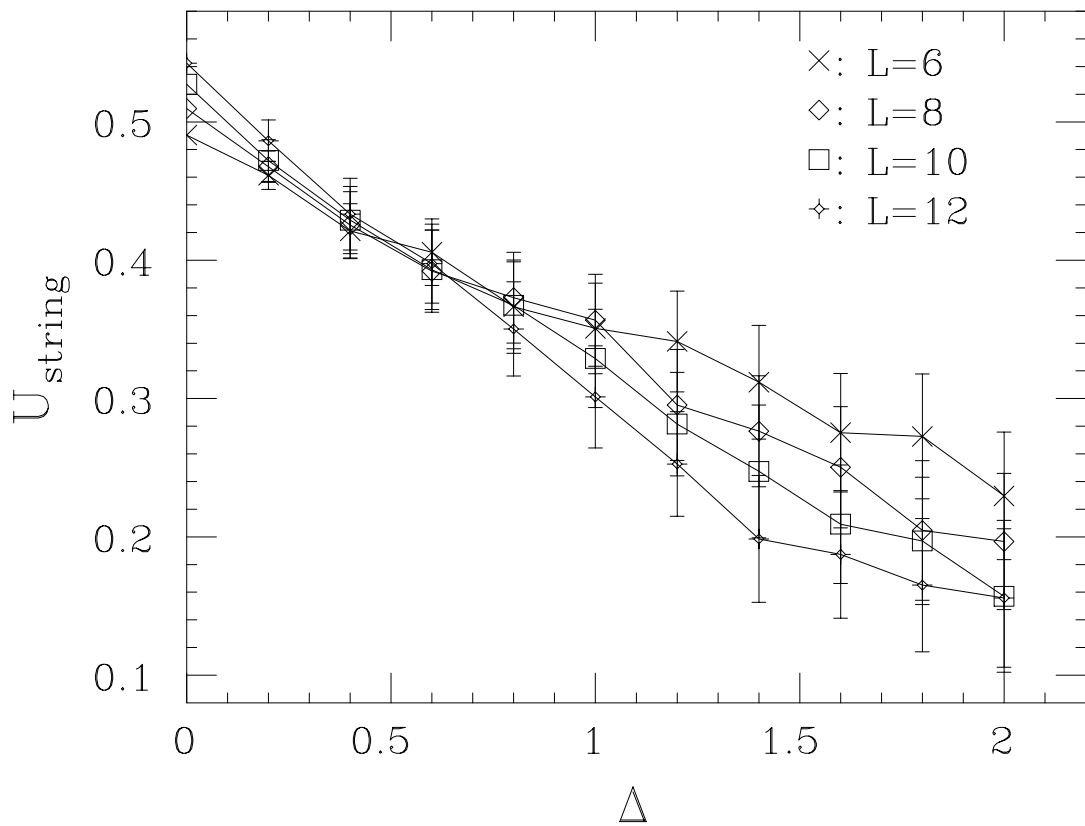


Figure 2: Plot of the Binder parameter (8) associated with the string order (7) with the randomness  $\Delta$  varied at the isotropic point  $\lambda = 1$ . The system-size-invariant point indicates the location of the critical point.

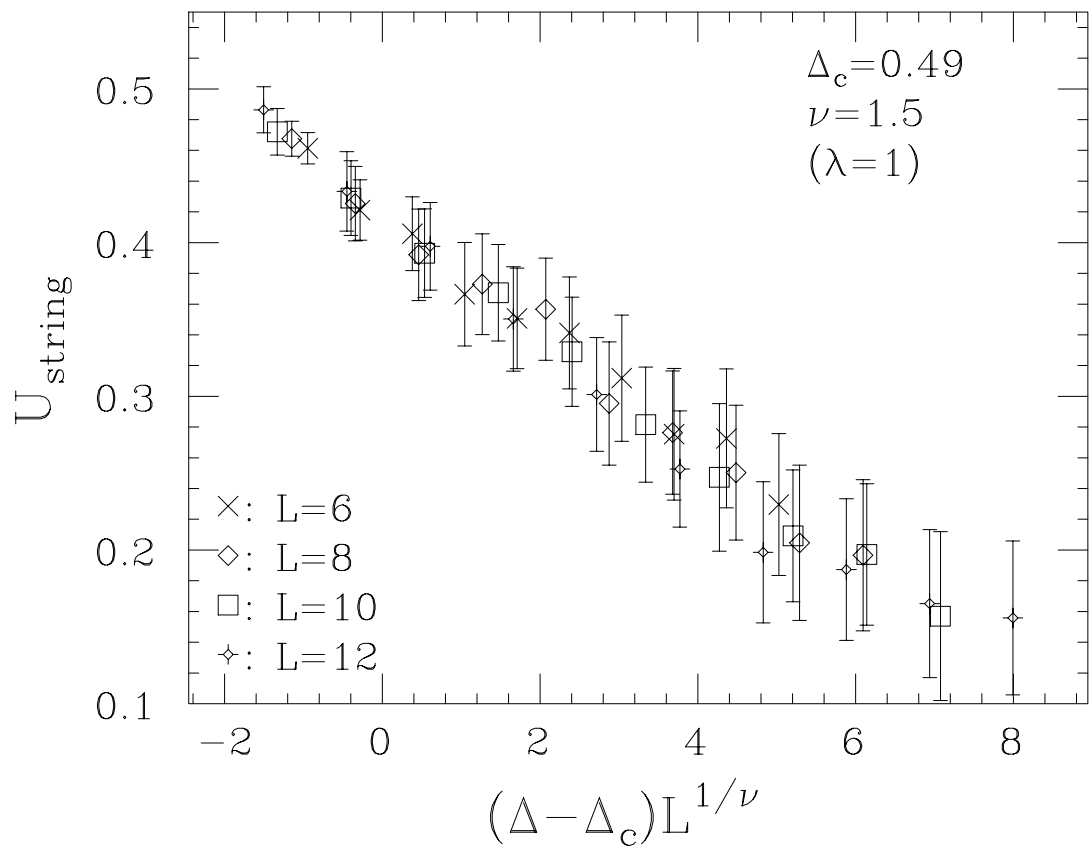


Figure 3: The scaling plot of the data shown in Fig. 2. This plot yields the estimates  $\Delta_c = 0.49 \pm 0.15$  and  $\nu = 3.4 \pm 2.2$ .

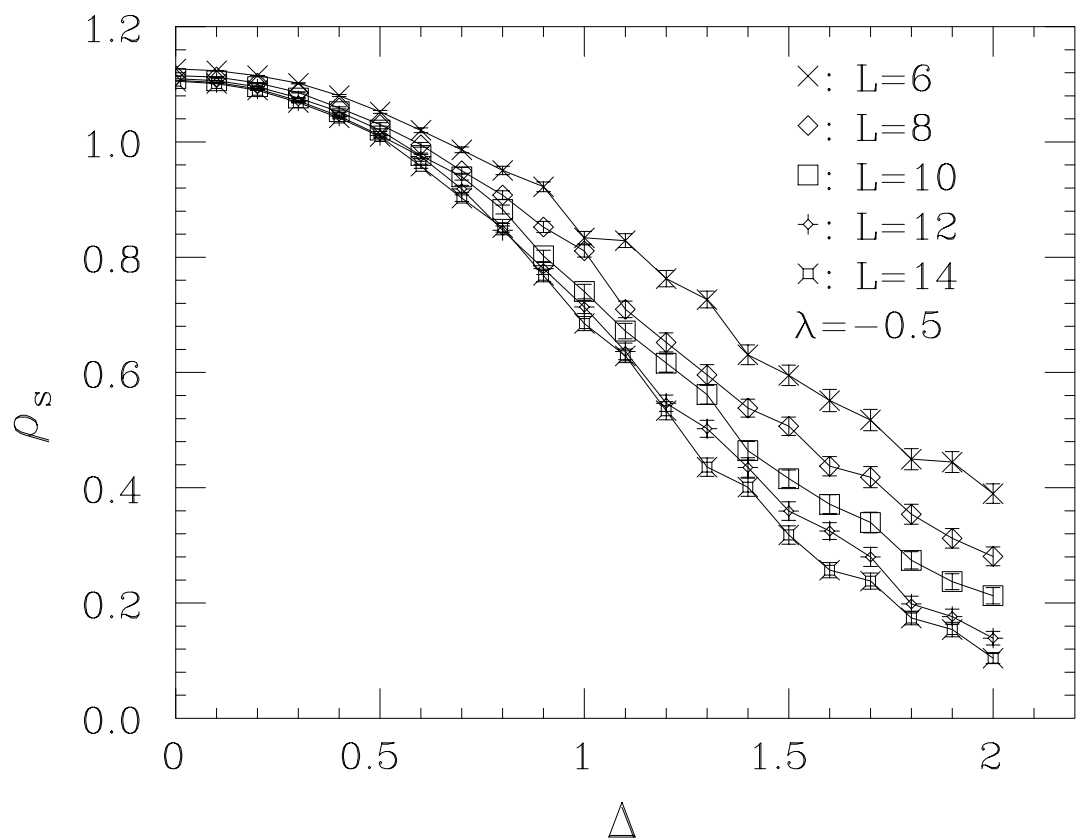


Figure 4: Plot of the spin stiffness (12) against the randomness at  $\lambda = -0.5$ .

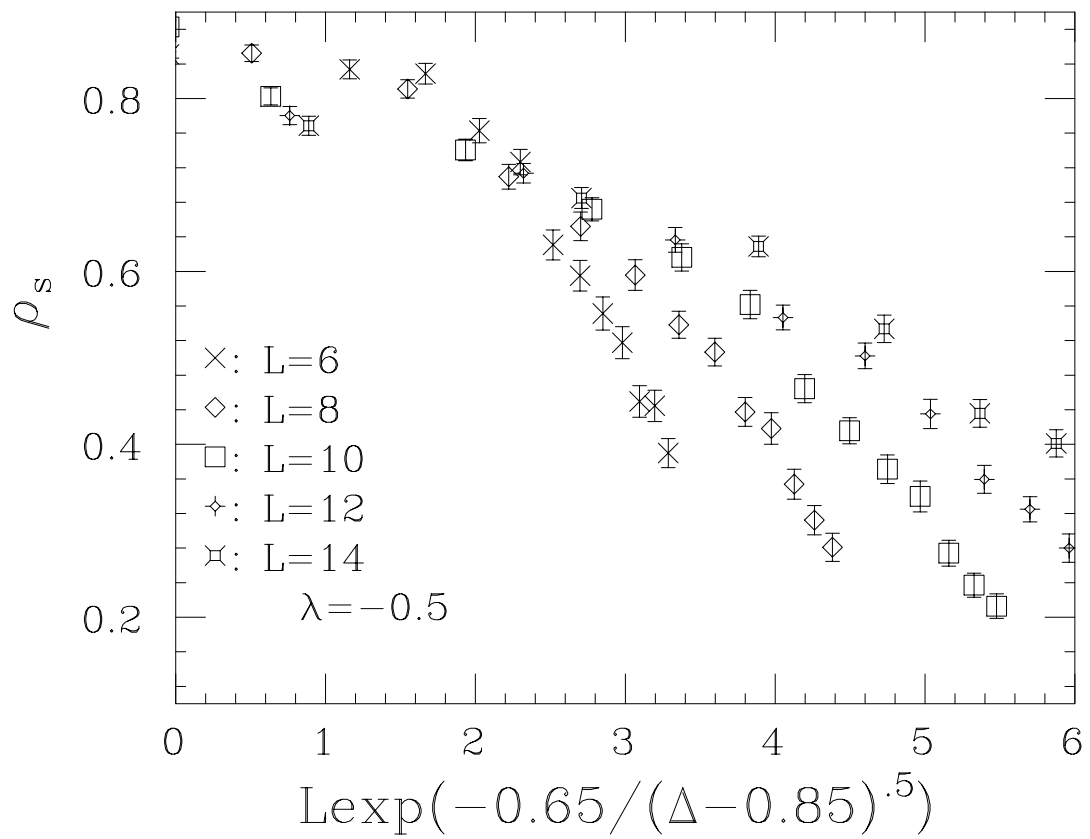


Figure 5: Scaling plot of the data shown in Fig. 4. This plot yields the estimate  $\Delta_c = 0.85 \pm 0.30$ .

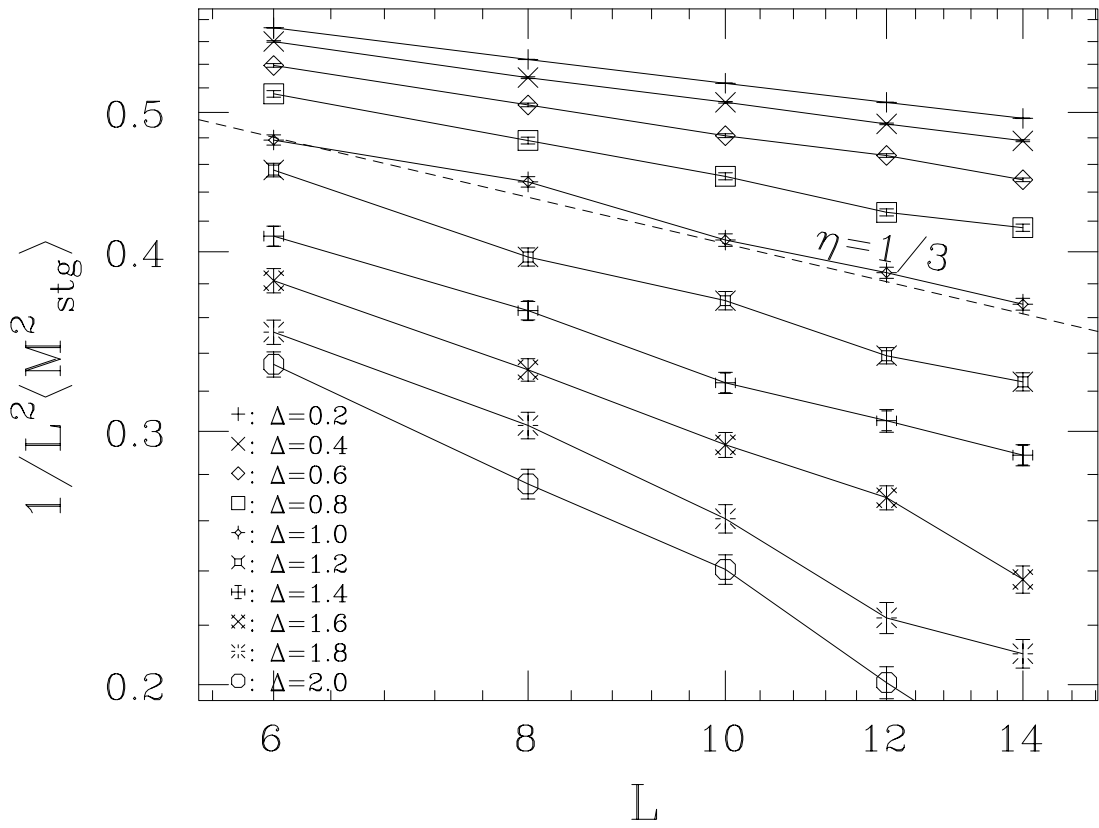


Figure 6: The square of the staggered magnetic moment (15) is plotted for various randomnesses at  $\lambda = -0.5$ . The dashed slope shows the decay rate  $\eta_c = 1/3$ , which is proposed for the criterion for the localization-delocalization transition.

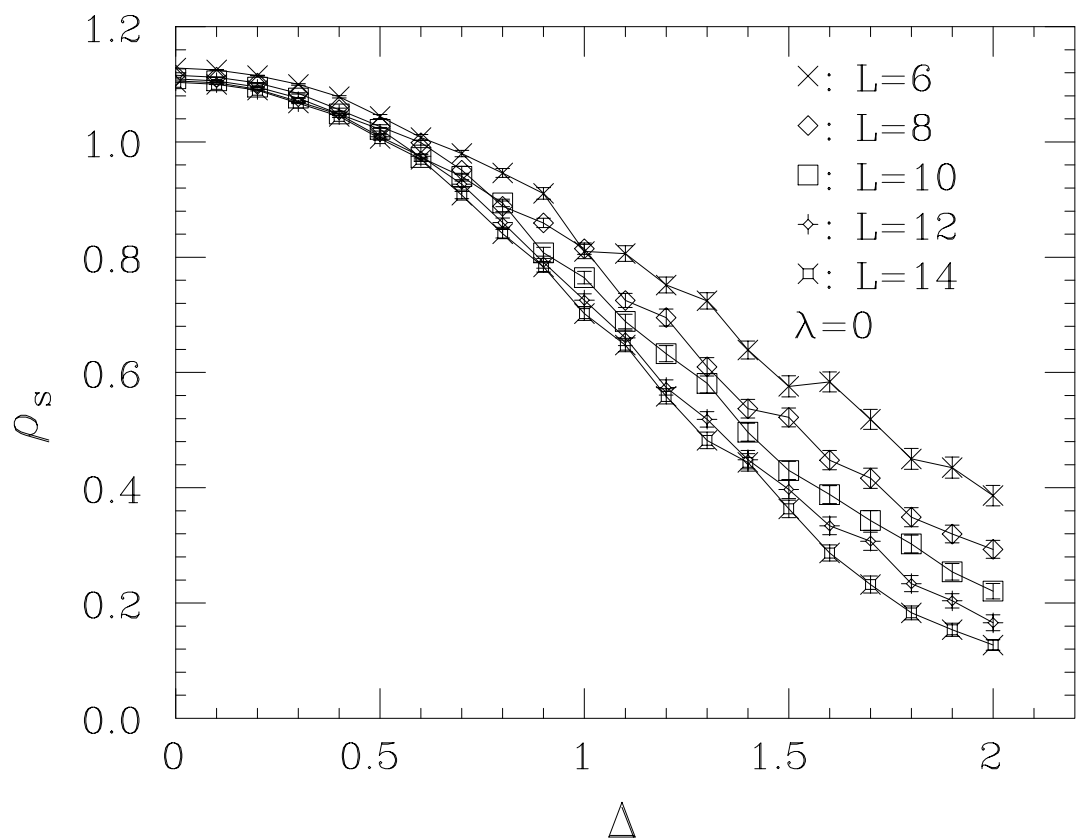


Figure 7: Plot of the spin stiffness (12) against the randomness at  $\lambda = 0$ .

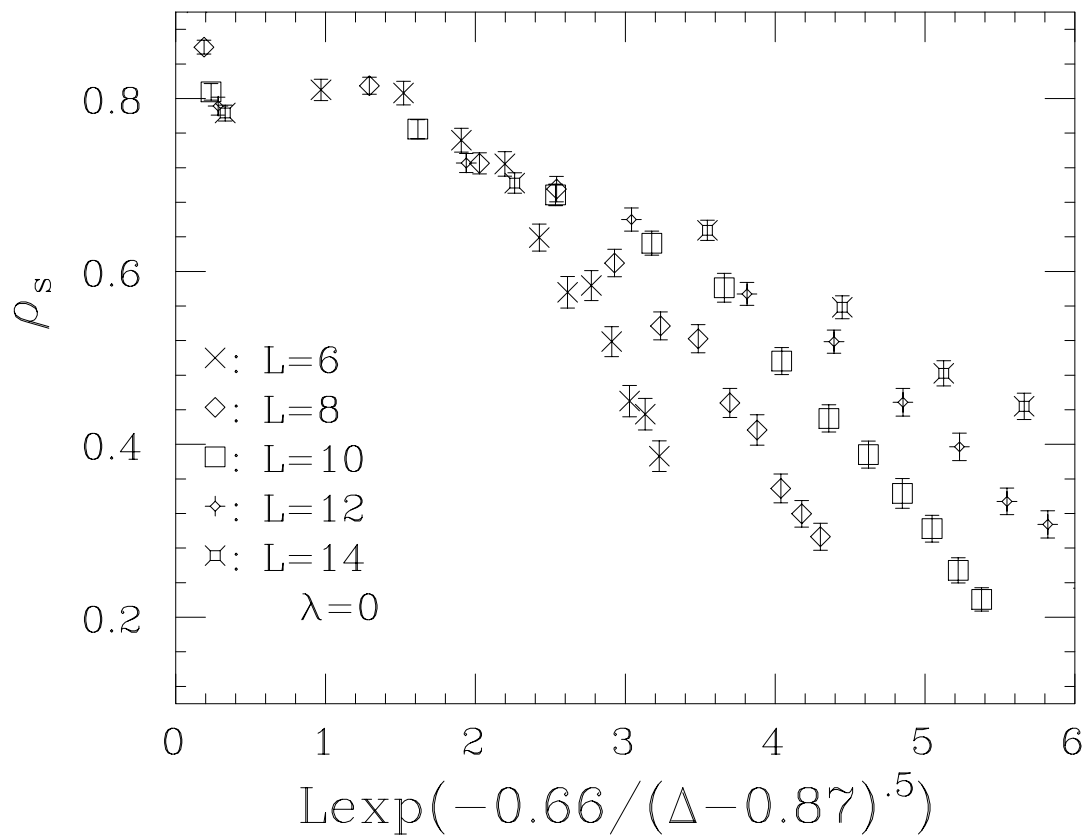


Figure 8: Scaling plot of the data shown in Fig. 7. This plot yields the estimate  $\Delta_c = 0.87 \pm 0.30$ .

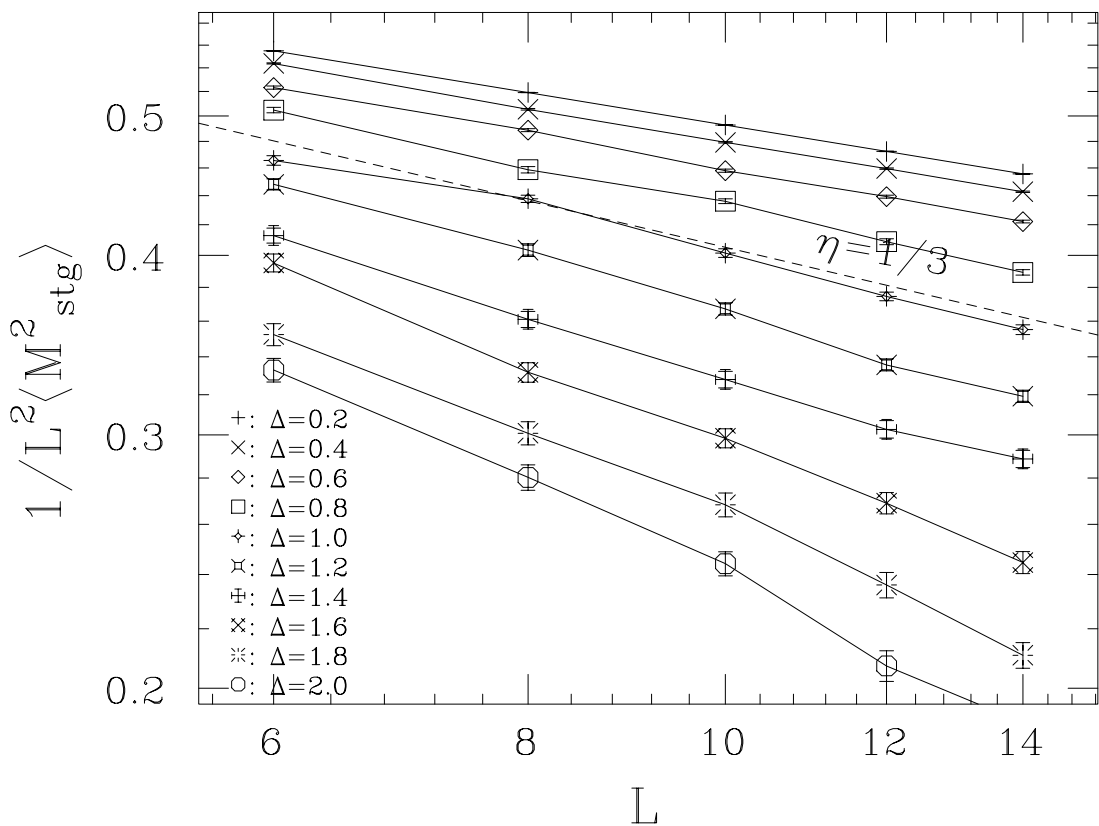


Figure 9: The square of the staggered magnetic moment (15) is plotted for various randomnesses at  $\lambda = 0$ . The dashed slope show the decay rate  $\eta_c = 1/3$ .

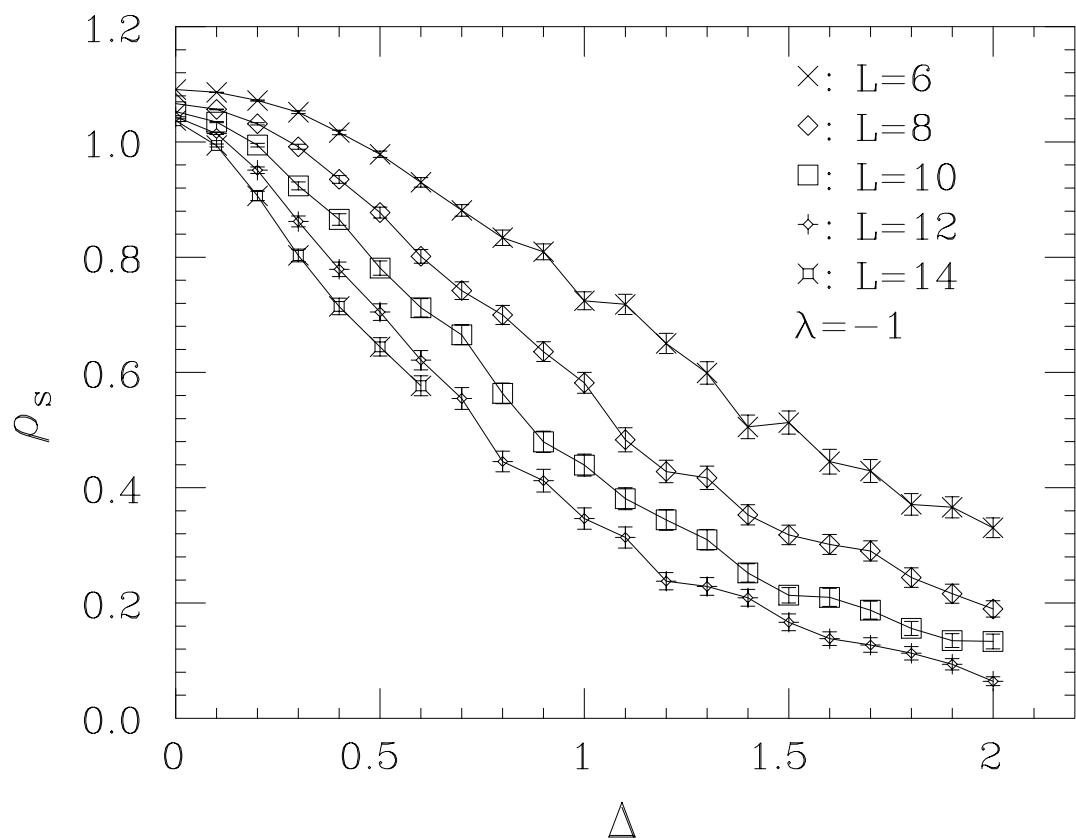


Figure 10: Plot of the spin stiffness (12) against the randomness at  $\lambda = -1$ .

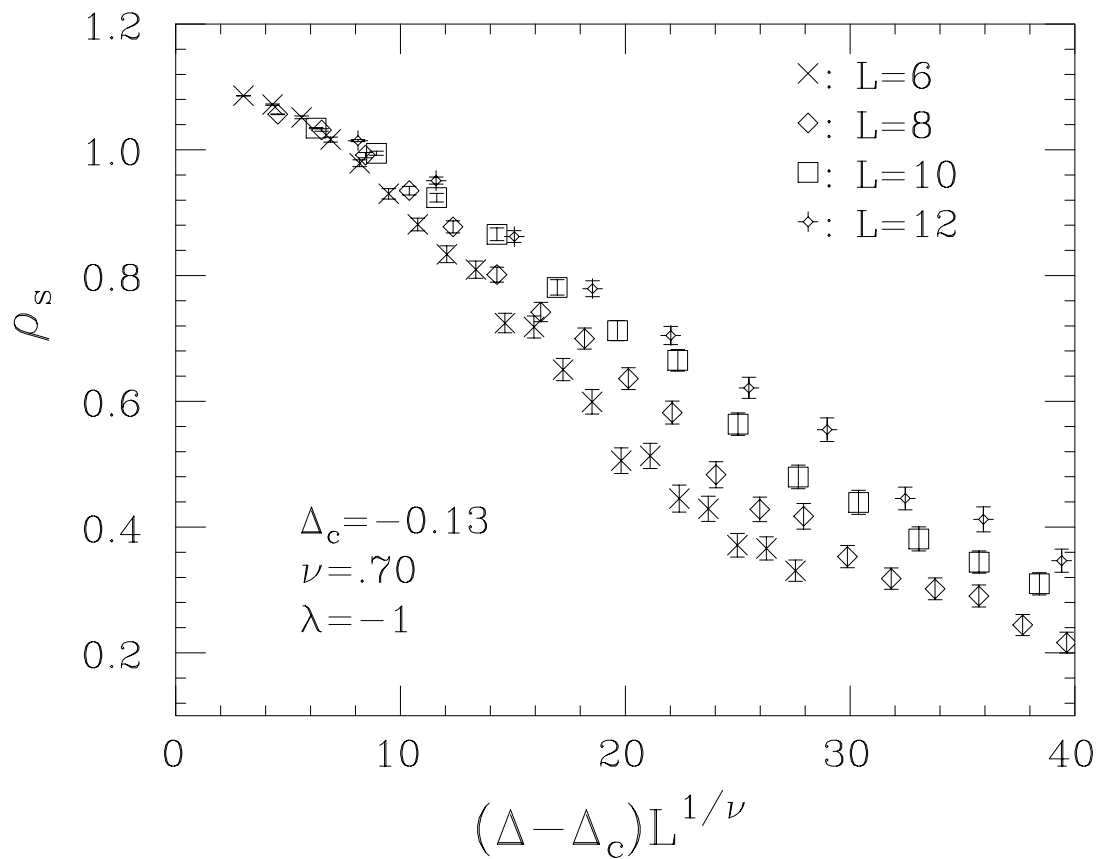


Figure 11: Scaling plot of the data shown in Fig. 10. This plot yields the estimate  $\Delta_c = -0.13 \pm 0.10$ .

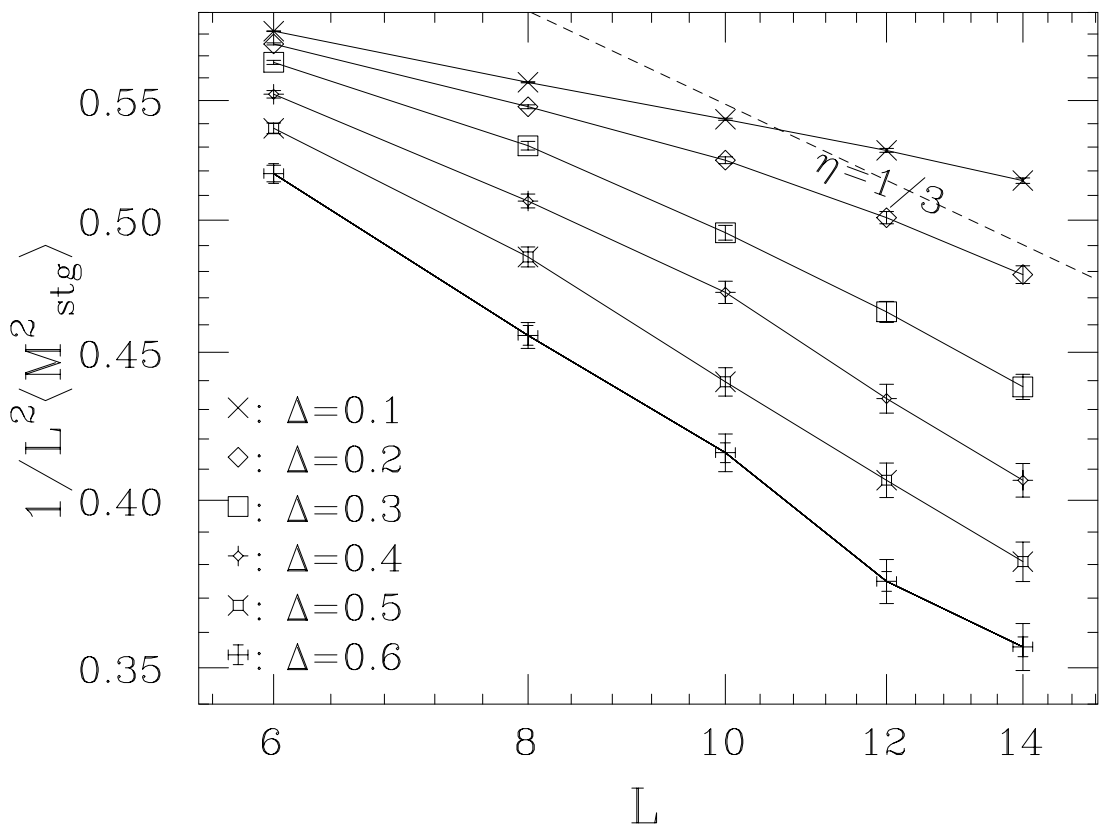


Figure 12: The square of the staggered magnetic moment (15) is plotted for various randomnesses at  $\lambda = -1$ . The dashed slope show the decay rate  $\eta_c = 1/3$ .

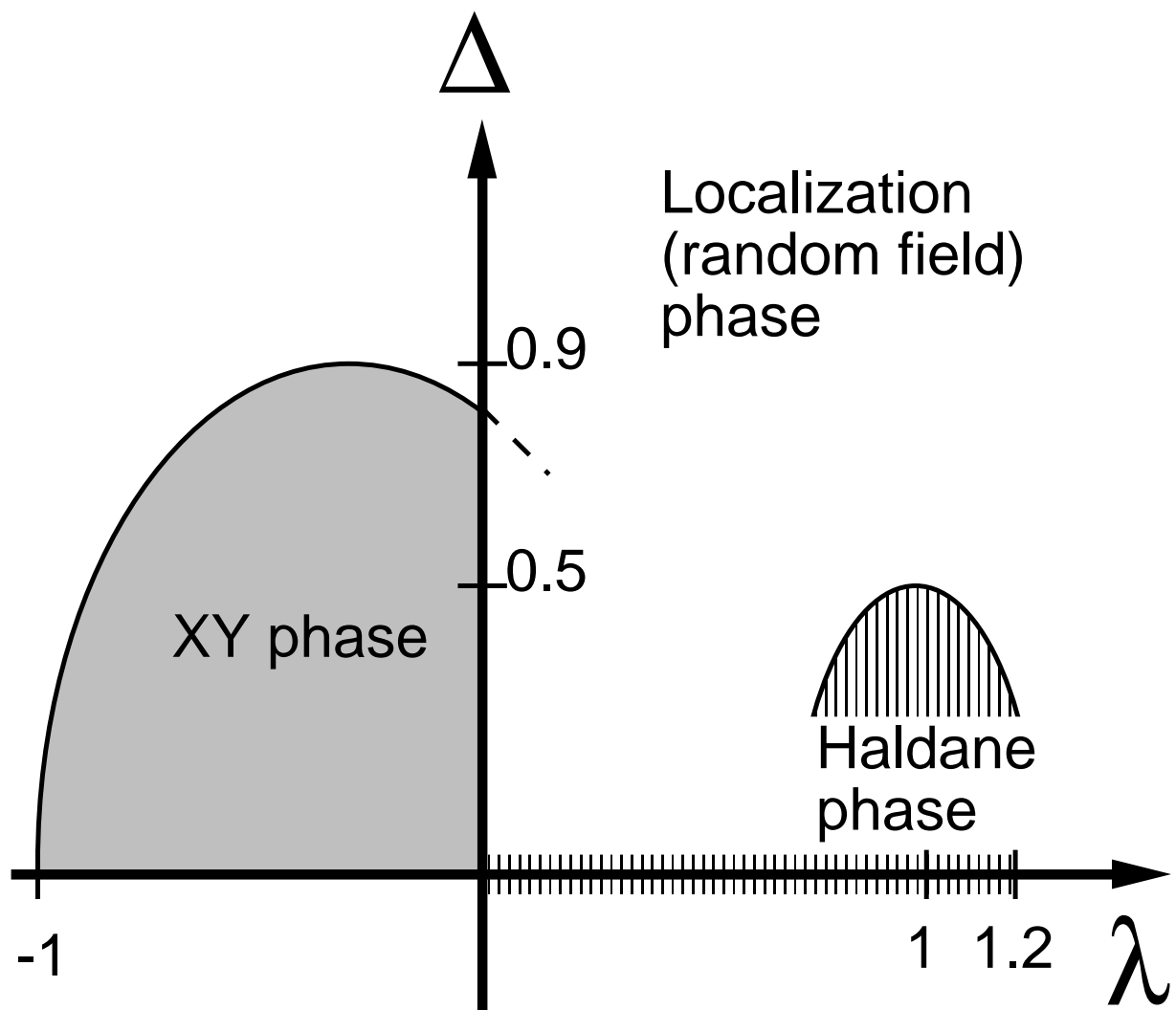


Figure 13: Phase diagram of the  $S = 1$   $XXZ$  model with the random magnetic field; the Hamiltonian is given by eq. (1).

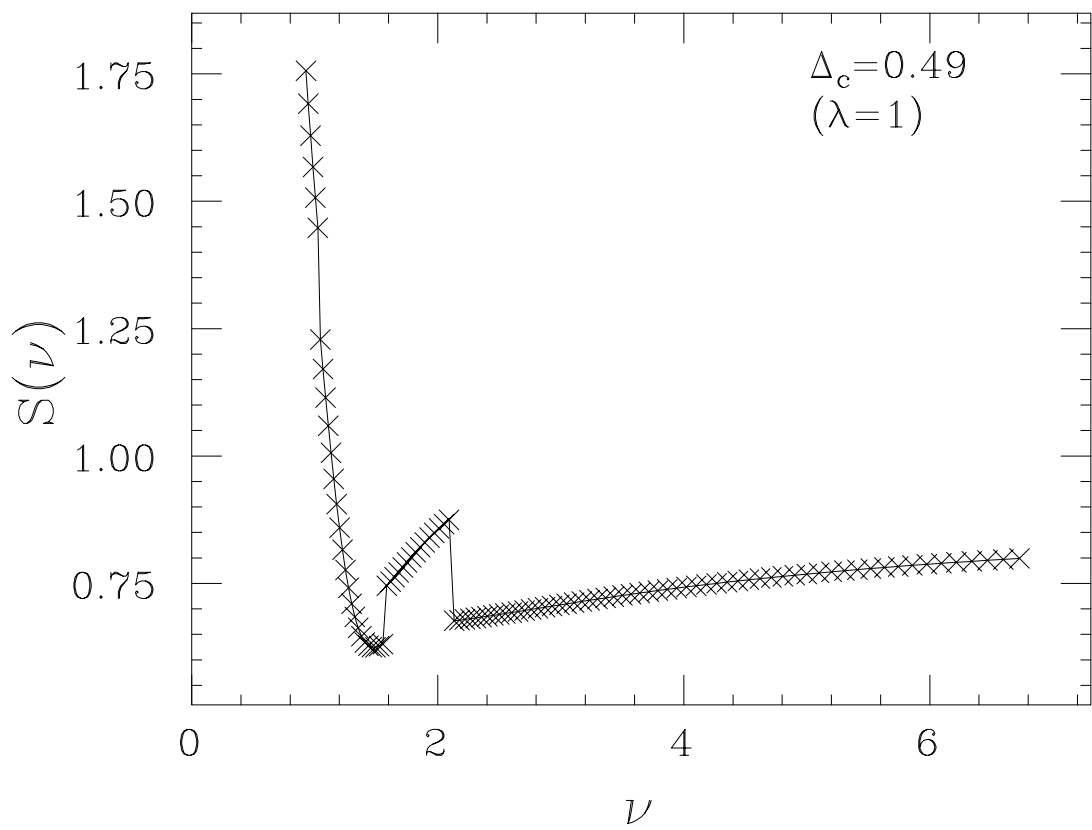


Figure 14: Local linearity function  $S$  (16) for the scaling data shown in Fig. 3 is plotted for various trial values of  $\nu$  with  $\Delta_c = 0.49$  fixed. The location of the minimum yields the estimate of the exponent  $\nu \sim 1.5$ .